Prognostic prediction of patients having classical papillary thyroid carcinoma with a 4 mRNA-based risk model

Lin Xiang, MS[a], Jun-Hui Zhao, MS[a], Yao Tang, MS[a], Jun-Wu Tan, MS[a], Liang-Bo Li, MS[a], Cheng Gong, MS[a],*

Abstract

The dysregulation of protein-coding genes involved in various biological functions is closely associated with the progression of thyroid cancer. This study aimed to investigate the effects of dysregulated gene expressions on the prognosis of classical papillary thyroid carcinoma (cPTC). Using expression profiling datasets from the Cancer Genome Atlas (TCGA) database, we performed differential expression analysis to identify differentially expressed genes (DEGs). Cox regression and Kaplan–Meier analysis were used to identify DEGs, which were used to construct a risk model to predict the prognosis of cPTC patients. Functional enrichment analysis unveiled the potential significance of co-expressed protein-encoding genes in tumors. We identified 4 DEGs (SALL3, PPBP, MYH1, and SYNDIG1), which were used to construct a risk model to predict the prognosis of cPTC patients. These 4 genes were independent of clinical parameters and could be functional in cPTC carcinogenesis. Furthermore, PPBP exhibited a strong correlation with poorer overall survival (OS) in the advanced stage of the disease. This study suggests that the 4-gene signature could be an independent prognostic biomarker to improve prognosis prediction in cPTC patients older than 46.

Abbreviations: cPTC = classical papillary thyroid carcinoma, DEGs = differentially expressed genes, FDR = false discovery rate, OS = overall survival, TCGA = the Cancer Genome Atlas.

Keywords: bioinformatics, classical papillary thyroid carcinoma, mRNAs, prognosis, risk mode

1. Introduction

Thyroid cancer, specifically papillary thyroid cancer, has seen a significant increase in incidence over the last 3 decades,[1] with an estimated 52,000 new cases reported in the United States in 2019.[2] Despite this increase, mortality rates for thyroid cancer have remained relatively constant at <2% over the past half-century.[3] In China, a rapidly increased incidence of thyroid cancer, but a steady trend in mortality rate was also found. The increased incidence of thyroid cancer was mainly reported as papillary thyroid cancer with a maximum tumor diameter of <1 cm.[4] Despite the high 10-year survival rate of thyroid cancer patients, the prognosis for patients with high-risk disease remains poor.[5,6] The major challenge in managing thyroid cancer is accurately identifying the patients with advanced or high-risk disease, thereby reducing the possibility of overtreatment of the patients with low-risk disease, especially in older patients with classical papillary thyroid carcinoma (cPTC).[7] For this purpose, prognostic prediction with molecular analysis methods, such as the detection of mRNA expression, is significant. Additionally, aging is an essential factor that impacts the prognosis of the thyroid.

To better understand the aberrant gene expression in cPTC, this study aims to identify novel molecular biomarkers that can effectively predict the clinical outcomes of patients with cPTC. The strategy of this study is to use the RNA expression profiles of the cPTC patients, which were obtained from the Cancer Genome Atlas (TCGA) database and used to develop a prognostic risk score system to stratify patients into 2 groups with significantly different overall survival (OS). This approach is essential for older patients, where accurate prognosis prediction is crucial to avoid overtreatment.

2. Materials and methods

2.1. Acquisition of expression profiling data and corresponding information of cPTC patients

Gene expression profiling data of 406 tissue samples of cPTC and 58 normal tissue samples, including their corresponding clinical information, was retrieved from the TCGA database

[a] Department of Otolaryngology-Head and Neck Surgery, Minda Hospital of Hubei Minzu University, Enshi, Hubei, China.

* Correspondence: Cheng Gong, Department of Otolaryngology-Head and Neck Surgery, Minda Hospital of Hubei Minzu University, No.2, Wufeng Mountain Road, Tuqiao Avenue, Enshi, Hubei 445000, China (e-mail: gongcheng202104@163.com).

(https://cancergenome.nih.gov/). Genetic annotation files were downloaded from the Gencode Database (https://www.gencodegenes.org/human/release_22.html), which is a bioinformatics tool to identify all gene features in the human genome using a combination of computational analysis, manual annotation, and experimental validation. Our study followed the publication guidelines and data access policies of TCGA (http://cancergenome.nih.gov/pulications/publicationguidelines).

2.2. Analysis of differentially expressed genes (DEGs)

The DEGs (mRNAs) between tumor tissues of the cPTC patients and normal tissues were identified by "edgeR" package of R software (v4.0.3), based on the screening criteria: Log2FC of thresholds > 1.0 and a false discovery rate (FDR) threshold of < 0.01. The low-abundance genes were removed before analysis according to the following criteria: expression raw count value > 0 in more than 30% of samples and count per million (CPM) > 1 among at least 3 samples. The mRNA expression level of samples was converted to Fragments Per Kilobase of exon model per million mapped fragments (FPKM), which was used for the subsequent analysis.

2.3. Construction and validation of the risk model

The dataset from TCGA was used to construct and validate the risk model, in which the cPTC patients with at least 30 days of OS were included and randomized into training cohorts and validation groups for survival analysis. The independent predictors of prognosis were identified by both univariate Cox regression analysis ($P < .005$ as its threshold) and multivariate Cox regression analysis ($P < .05$ as its threshold). Based on the expression levels of identified genes/mRNAs, a risk score formula for patients' survival prediction was designed. Moreover, the construction and visualization of the risk model using R packages and the risk score were determined by analyzing the results of a multivariate Cox regression model that can divide patients into low- and high-risk groups based on their median risk score. The relationship of the identified mRNAs with the OS of patients was evaluated by Kaplan–Meier survival analysis and the log-rank test. The time-dependent receiver operating characteristic (ROC) curve within 10 years was utilized to evaluate the risk model sensitivity and specificity in survival prediction. Finally, the correlation of the mRNAs signature-dependent survival prediction with clinical parameters was evaluated by multivariate Cox regression analysis, the results of which were shown as forest plots. Principal component analysis was also used to assess the effectiveness of this risk model.

2.4. Functional enrichment analysis

The Pearson correlation coefficient (r) was computed between at least one prognostic mRNA and protein-coding genes utilizing their expression values to construct co-expression networks, with a threshold set at $P < .01$ and a coefficient >0.04. Gene ontology (GO) and Kyoto encyclopedia of genes and genomes (KEGG) analyses were conducted using the clusterProfiler package[8] to delineate the functional roles of co-expression mRNAs. Available online: http://geneontology.org/, https://www.genome.jp/kegg/. The enrichment analysis of identified genes/mRNAs was performed by the KEGG pathway and the potential GO (Gene Ontology) terms based on the lowest over-represented P value ($P < .01$).

We employed co-expressed genes to construct protein-protein interaction (PPI) networks in the STRING database (v11.5, https://cn.string-db.org/) with high confidence. Subsequently, hub genes analysis and visualization were conducted using the cytoHubba[9] package of Cytoscape[10] (v3.6.1) software within the PPI networks. The top 10 nodes were selected as hub genes based on their degree scores. References: Available online: https://apps.cytoscape.org/apps/cytohubba, Available

online: https://cytoscape.org/. The pathways related to the Hallmark genes were identified by Gene Set Enrichment Analysis (GSEA) software (v4.0.3), using "h.all.v7.5.symbols.gmt" of MSigDB with a threshold ($P < .05$).

2.5. Statistical analysis

Pearson correlation coefficient (r) was used for evaluating the relationship between clinical parameters and expression levels of identified genes/mRNAs. An independent t-test was used to test the statistical difference between the 2 subgroups in the comparison. The results of the analysis were visualized by line charts and box diagrams. The numbers of stars indicate the levels of significance in statistical analysis (*$P < .05$, **$P < .01$, ***$P < .001$, and ****$P < .0001$).

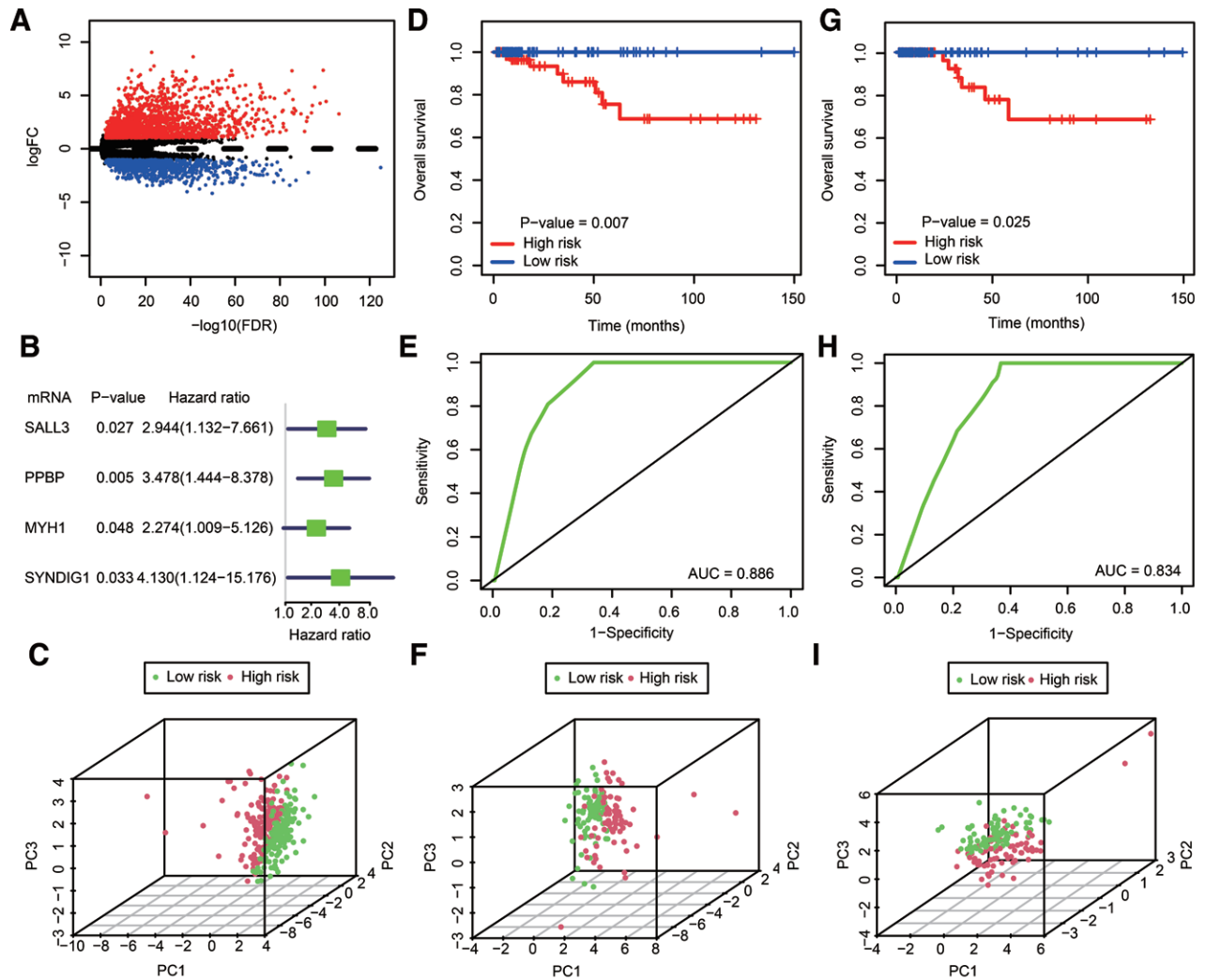## 3. Results

3.1. Expression profiles and DEGs/mRNAs

A total of 406 cPTC cases with profile data of protein-coding genes were extracted from the TCGA database. The Gencode database annotated 19,712 genes/mRNAs. Among those 19,712 genes, 2848 DEGs or mRNAs between cPTC and adjacent normal tissues were identified. As shown in Figure 1A, the distribution of all significant DEGs was described by a Volcano plot of the FDR (-log10FDR) and expression ratio (log2FC).

3.2. Construction of survival-associated RNAs and prognostic signatures

Through Cox regression and Kaplan–Meier analysis of 2848 identified DEGs, 4 DEGs (SALL3, PPBP, MYH1, and SYNDIG1) were identified in Table 1, which were significantly associated with poorer OS in 309 patients whose OS was at least 30 days (Fig. 1B). Next, based on the median cutoff point of these 4 identified mRNAs, 158 cases were classified into the high-risk group and other 151 cases into the low-risk group. Kaplan–Meier survival analysis and the log-rank test showed that the survival rate of those in the high-risk group was significantly shorter than those in the low-risk group in both the training set (Fig. 1D, $P = .007$) and testing set (Fig. 1G, $P = .025$). Relied on 4 identified mRNA signature-based models, the area under the time-dependent ROC curve (AUC) in the training and testing sets was calculated as 0.886 (Fig. 1E) and 0.834 (Fig. 1H), respectively. The distribution of patients in different groups is shown in Figure 1C (entire set), 1F (training set), and 1I (testing set). Moreover, the survival status, risk score, heatmap, and expression profiles of 4 identified mRNAs were presented in Figure 2, indicating that the clinical outcomes of patients in the low-risk group are better than those in the high-risk group, while the expression level of 4-mRNAs in the high-risk group was higher than that in the low-risk group. Finally, after adjusting clinical parameters by Cox regression analysis, we found that the risk score calculated based on the 4-mRNA signature was still tightly associated with survival in either the training (Fig. 3A–B) or the testing set (Fig. 3C–D). Furthermore, the prognostic value of the 4-mRNA signature was independent of either age or AJCC stage, according to Kaplan–Meier survival analysis (Fig. 4).

3.3. Functional enrichment and Hub mRNAs of co-expression genes

A total of 1179 co-expressed protein-coding genes were identified and utilized for enrichment analysis and construction of protein-protein interaction (PPI) networks. Our study revealed that GO terms were enriched in various biological processes (Fig. 5A), such as muscle system process, actin binding, etc. Additionally, KEGG pathway analysis showed that the

Figure 1. Construction of the prognostic model based on survival-related mRNAs. (A) Volcano plot of differentially expressed mRNAs. (B) Forest plot of the univariable Cox regression analysis results of mRNA signature. (D and G) Kaplan–Meier curves of OS of the cPTC patients in the training set (D) and testing set (G), using the 4-mRNA prognostic model. (E and H) The area under the time-dependent ROC curve (AUC) in the training set (E) and testing set (H). (C, F, and I) PCA plot of the cPTC patients in the entire set (C), training set (F), and testing set (I), according to analysis using the prognostic model. cPTC = classical papillary thyroid carcinoma, PCA = principal component analysis.

Table 1

The expression profiles of 4 prognostic signatures.

Symbol	Tissue	Mean FPKM	logFC	P value	FDR
SALL3	Tumor	0.089	2.816	<.001	<0.001
	Normal	0.013			
PPBP	Tumor	1.175	1.572	<.001	<0.001
	Normal	0.422			
MYH1	Tumor	0.046	2.494	.001	0.002
	Normal	0.008			
SYNDIG1	Tumor	1.333	-1.836	<.001	<0.001
	Normal	4.993			

FDR = false discovery rate, MYH1 = myosin heavy chain 1, PPBP = pro-platelet basic protein, SALL3 = spalt-like transcription factor 3, SYNDIG1 = synapse differentiation-inducing 1.

calcium signaling pathway was mostly associated with these genes (Fig. 5B). Additionally, several genes, including MYL1, TTN, ACTN2, and RUVBL1, were identified as hub genes in the PPT network (Fig. 5C). The expression profiles of the top 10 hub genes are depicted in Figure 6. We also found that epithelial-mesenchymal transition and Kras-related signaling pathways were significantly enriched in the high-risk group (Fig. 5D and E).

3.4. Correlation of clinical traits with gene expression profiles

Kaplan–Meier survival analysis suggested that pro-platelet basic protein (PPBP) was closely correlated with poorer OS (Fig. 7A). The expression of PPBP was upregulated in the advanced stage of the disease, compared with that in the low clinical stage (T stage shown in Fig. 7B and AJCC stage shown in Fig. 7C, respectively).

4. Discussion

Despite extensive molecular studies, thyroid cancer is a common disease with unclear etiology and pathogenesis.[11] The increasing incidence of papillary thyroid cancer highlights the importance of accurate prognosis prediction and avoidance of unnecessary treatment.[1] Our study identified 2848 mRNAs associated with cPTC compared to normal tissue. Using a 4-mRNA prognostic signature (SALL3, PPBP, MYH1, SYNDIG1), we developed a risk score model to predict the survival of the cPTC patients, particularly those over 46 years old. Our analysis found that high-risk patients had poorer prognoses, and we could predict a 10-year survival time. The efficacy of our prediction was
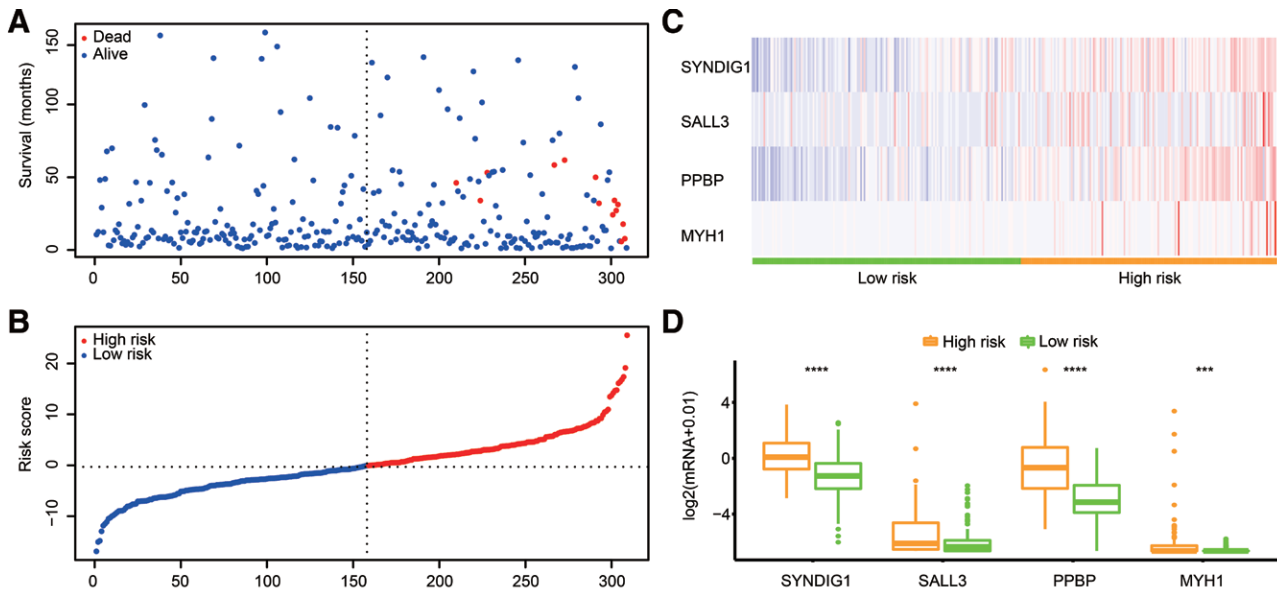
Figure 2. Assessment of prognostic signatures in training sets. (A and B) Distribution of the patients' survival status and risk score. (C and D) Heatmap and box diagram of the 4 prognostic mRNAs.
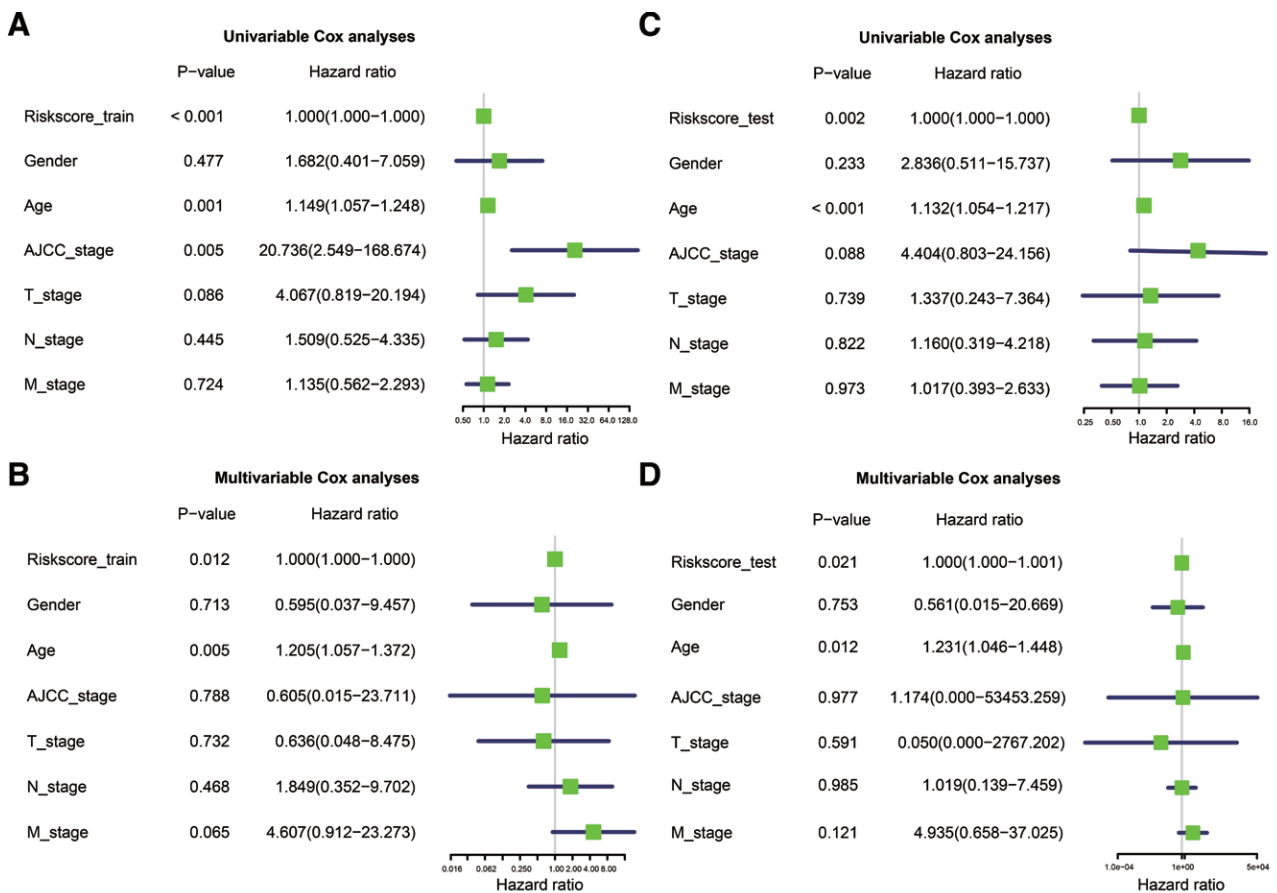
Figure 3. Independent validation of the 4-mRNA risk score model. Forest plot for 4-mRNA signature in the training set (A and B) and testing set (C and D), based on Cox regression analysis.

verified by multivariate Cox regression and subgroup analyses. Additionally, we identified PPBP as a factor closely linked with the AJCC stage, T stage, and survival status. GSEA showed that the high-risk group was significantly enriched in epithelial-mesenchymal transition and Kras-related signaling pathways.

Identifying effective prognostic biomarkers and exploring potential regulatory networks are vital for developing tailored treatment options for patients with thyroid cancer. Current data suggests that surveillance and overdiagnosis play a significant role in the increasing incidence of thyroid cancer.[12] Several
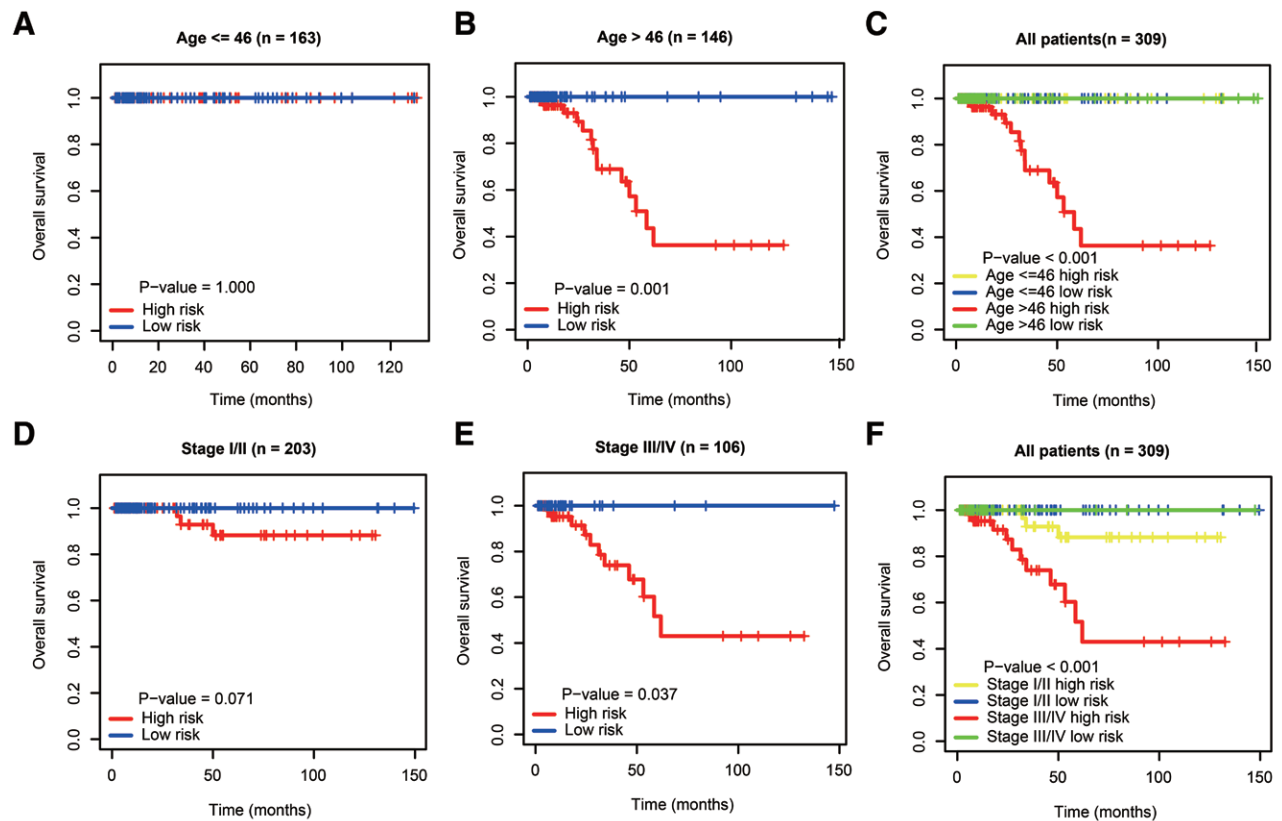
Figure 4. Stratification analyses of the patients' OS which was adjusted to the age and stage using the 4-mRNA signature in the entire set. (A–C) Kaplan–Meier curves of the age cohort based on the risk model. (D–F) Kaplan–Meier curves of the stage cohort based on the risk model. OS = overall survival.

studies have attempted to develop prognostic models using different sets of genes, with varying degrees of success, such as a 7-mRNA prognostic signature model (AUC = 0.792) based on immune-related genes.[13] Our findings suggest that SALL3, PPBP, MYH1, and SYNDIG1 may be effective prognostic biomarkers for cPTC patients. SALL3, PPBP, and MYH1 exhibited high expression levels in tumor tissues, consistent with their expression in the high-risk group, indicating their potential role as oncogenes. However, the expression pattern of SYNDIG1 across different tissues was inconsistent with the survival analysis results. This suggests that SYNDIG1 may have a more complex effect on the occurrence and progression of thyroid cancer.

The Synapse Differentiation-Inducing 1 (SYNDIG1) gene encodes a type II transmembrane protein known to bind to the glutamate receptor alpha-amino-3-hydroxy-5-methyl-4-isoxazolepropionic acid (AMPA), thereby regulating excitatory synapse number and function.[14] Glutamate activation of the Kras-MAPK signaling pathway via AMPA receptors has increased pancreatic cancer cell invasion and migration.[15] Interestingly, recent studies have suggested that circulating glutamine can reduce the risk of thyroid cancer, rather than other types of cancers.[16] Glutamine is metabolized to glutamate in the human body,[17] and aberrant overexpression of Glutaminase, an enzyme involved in glutamine metabolism, has been observed in papillary thyroid cancer, leading to suppressed glutaminolysis and reduced mitochondrial respiration. This results in enhanced proliferative, migratory, and invasive abilities of papillary thyroid cancer cells.[18] Additionally, gliomas have been found to increase neuronal excitability through AMPA receptor-dependent synapses, thereby positively regulating tumor progression.[19,20] AMPA receptor antagonists have been shown to inhibit the extracellular signal-regulated kinase pathway and decrease survivin expression, thereby suppressing cancer growth.[21,22] Hence, SYNDIG1 may be associated with

glutamate, AMPA receptor, and Kras-MAPK signaling pathways, playing complex regulatory roles in tumorigenesis and progression.

The Spalt-like Transcription Factor 3 (SALL3) gene encodes a sal-like C2H2-type zinc-finger protein and has been associated with aberrant DNA methylation and abnormal placental development in mice.[23] Previous study has investigated the relationship between SALL3 methylation and cancer occurrence.[24] SALL3 promoter methylation has been correlated with poor survival in patients with head and neck cancer.[25] SALL3 expression has also been found to inhibit DNMT3A-mediated CpG island methylation in hepatocellular carcinoma.[26] However, similar to our study, Zhong et al indicated that high expression of SALL3 in the high-risk group of patients with cPTC suggests its association with poor prognosis.[27]

Myosin Heavy Chain 1 (MYH1) encodes skeletal muscle myosin heavy polypeptide 1 and has been identified as a candidate breast cancer gene.[28] High expression of MYH1, along with other genes, has been associated with shorter OS in patients with cervical cancer.[29] Small interfering RNAs targeting MYH1 induce cell death by increasing lysosomal volume, altering lysosomal localization, and reducing autophagic flux.[30] Additionally, lower expression of ACTN2 and MYH1 has been associated with longer OS time in patients with head and neck squamous carcinoma.[31]

ACTN2, MYL1, and TTN have been identified as hub genes involved in PPI network construction. ACTN2 is a direct target of the NF-κB subunit RelA and α-Actinin-2 heterotrimers in the nuclei of gastric cancer cells.[32] ACTN2 overexpression enhances cellular motility and invasion abilities in hepatocellular carcinoma.[33] Myosin Light Chain-1 (MYL1) may promote cell migration through the epidermal growth factor (EGF)/EGF receptor (EGFR) signaling pathway and is significantly associated with the tumor immune microenvironment in head and
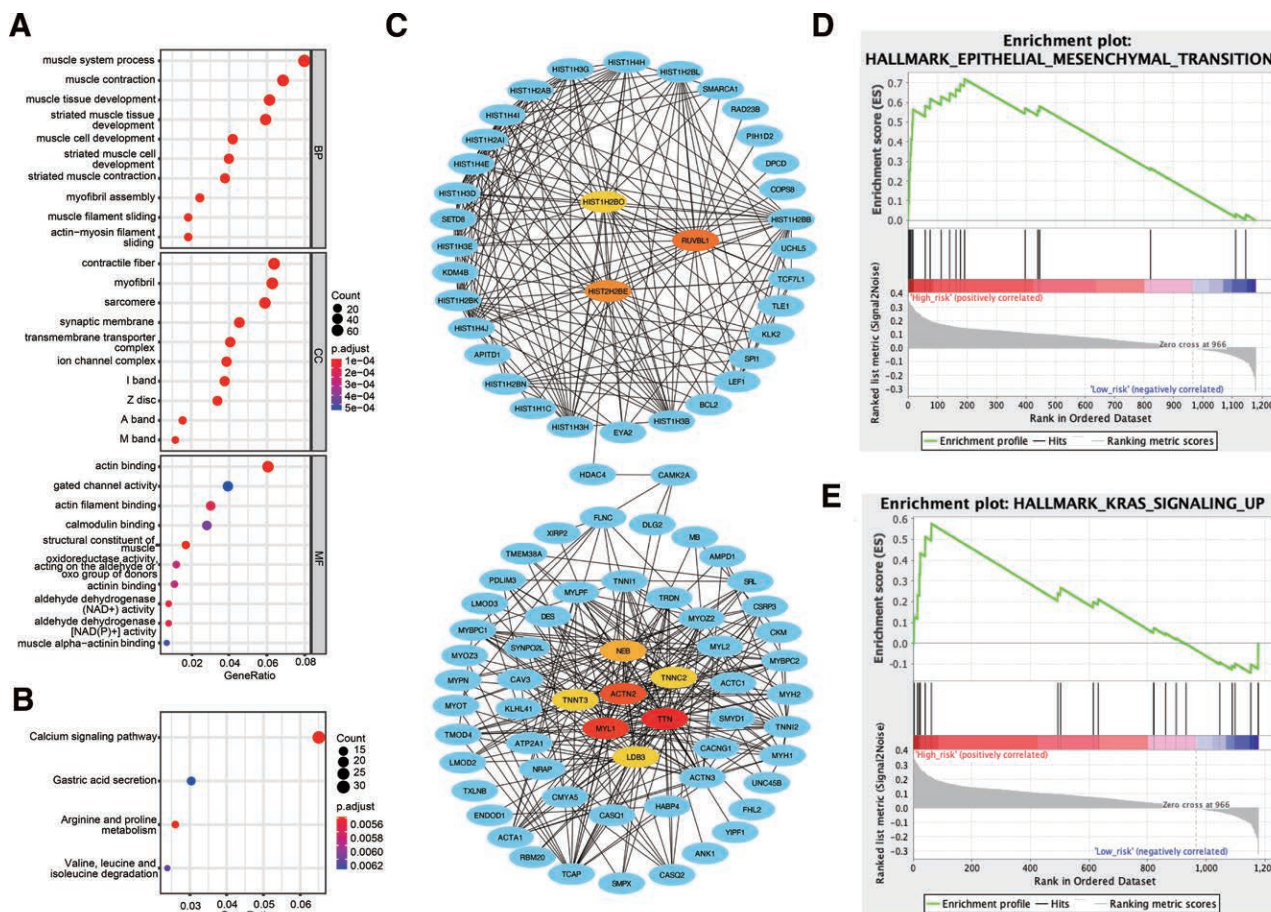
Figure 5. Functional enrichment of the co-expressed protein-coding genes of 4-mRNAs. (A and B) Distribution of enrichment map of the terms of GO (A) and KEGG (B). (C) Distribution of top 10 hub genes network. (D and E) Distribution of Hallmark genes-related pathways, according to GSEA analysis. GO = gene ontology, GSEA = Gene Set Enrichment Analysis, KEGG = Kyoto Encyclopedia of Genes and Genomes.
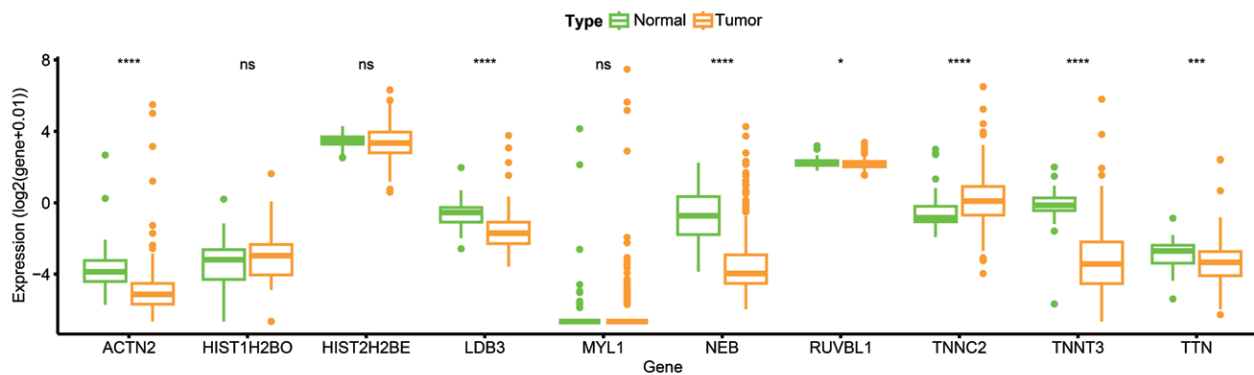

Figure 6. The expression profiles of top 10 hub genes.

neck squamous cell carcinoma.[34] MYL1 is also involved in the occurrence and development of prostate cancer by regulating muscle contraction, growth, and metabolism.[35] TTN mutations have the potential to modulate the tumor microenvironment to an immunosuppressive type and predict poor prognosis in patients with thyroid cancer.[36,37]

Pro-Platelet Basic Protein (PPBP) encodes a platelet-derived growth factor belonging to the CXC chemokine family. It has been reported to stimulate various cellular processes, including DNA synthesis and mitosis.[38] PPBP is associated with poor prognosis in colon cancer,[39] and it is also significantly increased

in lung cancer tissue. It is a novel diagnostic or prognostic biomarker and a potential therapeutic target.[40,41] PPBP formed stable interactions with GNG1l to drive non-small-cell lung cancer through chemokine signaling pathway.[42] Indeed, Colony Stimulating Factor 1 (CSF1) has been implicated in inducing monocyte expression and release of PPBP, promoting various aspects of breast cancer progression.[43] CSF1 has been shown to activate focal adhesion kinase (FAK) and induce matrix metalloproteinase 13 (MMP13) expression, contributing to breast cancer cell migration and invasion.[43] This highlights the multifaceted role of CSF1 and PPBP in the tumor microenvironment,
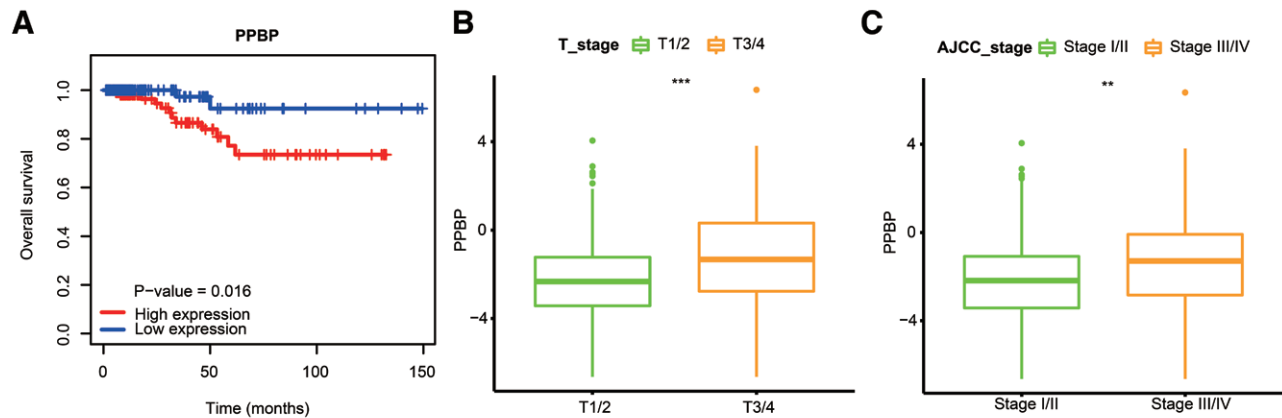
Figure 7. Relationships between clinical parameters and PPBP mRNA. (A) Kaplan–Meier curves for the entire cohort based on PPBP expression. (B–C) The expression level of PPBP in different T and AJCC stages. PPBP = pro-platelet basic protein.

where they can modulate immune cell recruitment, extracellular matrix remodeling, and tumor cell behavior to promote cancer progression.

Moreover, the PPBP/CXCR2 signaling pathway plays a crucial facilitating role in liver metastatic colorectal cancer and predicts poor prognosis.[44] However, the underlying mechanisms of PPBP in cancer development still require further investigation.

In our study, GSEA revealed that in the high-risk group, the co-expressed genes of the 4 identified mRNAs were primarily enriched in epithelial-mesenchymal transition (EMT) and Kras-related signaling pathways. EMT is a process commonly observed in the tumor microenvironment and has been associated with tumor progression and metastasis.[45,46] Furthermore, gene mutations in EMT and Kras are frequently observed in patients with papillary thyroid carcinoma,[47,48] suggesting the potential effectiveness of drugs targeted to Kras mutation.

However, several limitations should be acknowledged in this study. Firstly, our study primarily focuses on data extraction and analysis, which are based on methodology, and the results have not been verified by biological experiments or clinical specimens. Secondly, we analyzed and validated the 4 mRNA signatures for prognostic prediction, which only relied on the TCGA database, without additional expression data for further validation. Thirdly, although age[49,50] is known to be a prognostic factor for cPTC, the effect of age was not fully considered in our study. Finally, no experimental data are available on the potential mechanisms of SALL3, PPBP, MYH1, and SYNDIG1. Future experimental studies of these mRNAs will help us understand their functional roles in cPTC.

In conclusion, our study has identified SALL3, PPBP, MYH1, and SYNDIG1 as potentially effective prognostic biomarkers for predicting the survival of cPTC patients, particularly those over 46 years old. Moreover, PPBP may have the potential as a novel diagnostic or prognostic biomarker and potential therapeutic target in cPTC.

Acknowledgments

Author contributions

Conceptualization: Jun-Wu Tan, Liang-Bo Li.
Supervision: Cheng Gong.
Visualization: Lin Xiang.
Writing – original draft: Lin Xiang, Yao Tang.
Writing – review & editing: Lin Xiang, Jun-Hui Zhao.

References

[1] Seib CD, Sosa JA. Evolving understanding of the epidemiology of thyroid cancer. Endocrinol Metab Clin North Am. 2019;48:23–35.

[2] Siegel RL, Miller KD, Jemal A. Cancer statistics, 2019. CA Cancer J Clin. 2019;69:7–34.

[3] Lamartina L, Grani G, Durante C, et al. Follow-up of differentiated thyroid cancer - what should (and what should not) be done. Nat Rev Endocrinol. 2018;14:538–51.

[4] Du L, Wang Y, Sun X, et al. Thyroid cancer: trends in incidence, mortality and clinical-pathological patterns in Zhejiang Province, Southeast China. BMC Cancer. 2018;18:291.

[5] Links TP, van Tol KM, Jager PL, et al. Life expectancy in differentiated thyroid cancer: a novel approach to survival analysis. Endocr Relat Cancer. 2005;12:273–80.

[6] Suman P, Razdan SN, Wang CE, et al. Thyroid lobectomy for T1b-T2 papillary thyroid cancer with high-risk features. J Am Coll Surg. 2020;230:136–44.

[7] Haymart MR. Progress and challenges in thyroid cancer management. Endocr Pract. 2021;27:1260–3.

[8] Wu T, Hu E, Xu S, et al. clusterProfiler 4.0: a universal enrichment tool for interpreting omics data. Innovation (Camb). 2021;2:100141.

[9] Chin CH, Chen SH, Wu HH, et al. cytoHubba: identifying hub objects and sub-networks from complex interactome. BMC Syst Biol. 2014;8:S11.

[10] Shannon P, Markiel A, Ozier O, et al. Cytoscape: a software environment for integrated models of biomolecular interaction networks. Genome Res. 2003;13:2498–504.

[11] Xing M. Molecular pathogenesis and mechanisms of thyroid cancer. Nat Rev Cancer. 2013;13:184–99.

[12] Roman BR, Morris LG, Davies L. The thyroid cancer epidemic, 2017 perspective. Curr Opin Endocrinol Diabetes Obes. 2017;24:332–6.

[13] Lin P, Guo YN, Shi L, et al. Development of a prognostic index based on an immunogenomic landscape analysis of papillary thyroid cancer. Aging (Albany NY). 2019;11:480–500.

[14] Kalashnikova E, Lorca RA, Kaur I, et al. SynDIG1: an activity-regulated, AMPA- receptor-interacting transmembrane protein that regulates excitatory synapse development. Neuron. 2010;65:80–93.

[15] Herner A, Sauliunaite D, Michalski CW, et al. Glutamate increases pancreatic cancer cell invasion and migration via AMPA receptor activation and Kras-MAPK signaling. Int J Cancer. 2011;129:2349–59.

[16] Zhang K, Liang H. Genetic estimation of correlations between circulating glutamine and cancer. Am J Cancer Res. 2023;13:6072–89.

[17] Yoo HC, Yu YC, Sung Y, et al. Glutamine reliance in cell metabolism. Exp Mol Med. 2020;52:1496–516.

[18] Yu Y, Yu X, Fan C, et al. Targeting glutaminase-mediated glutamine dependence in papillary thyroid cancer. J Mol Med (Berl). 2018;96:777–90.

[19] Venkatesh HS, Morishita W, Geraghty AC, et al. Electrical and synaptic integration of glioma into neural circuits. Nature. 2019;573:539–45.

[20] Venkataramani V, Tanev DI, Strahle C, et al. Glutamatergic synaptic input to glioma cells drives brain tumour progression. Nature. 2019;573:532–8.

[21] Ruiz DS, Luksch H, Sifringer M, et al. AMPA receptor antagonist CFM-2 decreases survivin expression in cancer cells. Anticancer Agents Med Chem. 2018;18:591–6.

[22] Stepulak A, Sifringer M, Rzeski W, et al. AMPA antagonists inhibit the extracellular signal regulated kinase pathway and suppress lung cancer growth. Cancer Biol Ther. 2007;6:1908–15.

[23] Ohgane J, Wakayama T, Senda S, et al. The Sall3 locus is an epigenetic hotspot of aberrant DNA methylation associated with placentomegaly of cloned mice. Genes Cells. 2004;9:253–60.

[24] Misawa K, Kanazawa T, Mochizuki D, et al. Genes located on 18q23 are epigenetic markers and have prognostic significance for patients with head and neck cancer. Cancers (Basel). 2019;11:401.

[25] Misawa K, Mochizuki D, Imai A, et al. Epigenetic silencing of SALL3 is an independent predictor of poor survival in head and neck cancer. Clin Epigenetics. 2017;9:64.

[26] Shikauchi Y, Saiura A, Kubo T, et al. SALL3 interacts with DNMT3A and shows the ability to inhibit CpG island methylation in hepatocellular carcinoma. Mol Cell Biol. 2009;29:1944–58.

[27] Zhong LK, Gan XX, Deng XY, et al. Potential five-mRNA signature model for the prediction of prognosis in patients with papillary thyroid carcinoma. Oncol Lett. 2020;20:2302–10.

[28] Sjöblom T, Jones S, Wood LD, et al. The consensus coding sequences of human breast and colorectal cancers. Science. 2006;314:268–74.

[29] Deng Y, Song Y, Du Q, et al. Anti-HPV16 oncoproteins siRNA therapy for cervical cancer using a novel transdermal peptide PKU12. Front Oncol. 2023;13:1175958.

[30] Groth-Pedersen L, Aits S, Corcelle-Termeau E, et al. Identification of cytoskeleton-associated proteins essential for lysosomal stability and survival of human cancer cells. PLoS One. 2012;7:e45381.

[31] Ju G, Yao Z, Zhao Y, et al. Data mining on identifying diagnosis and prognosis biomarkers in head and neck squamous carcinoma. Sci Rep. 2023;13:10020.

[32] Wang C, Xie B, Yin S, et al. Induction of filopodia formation by α-Actinin-2 via RelA with a feedforward activation loop promoting overt bone marrow metastasis of gastric cancer. J Transl Med. 2023;21:399.

[33] Lo LH, Lam CY, To JC, et al. Sleeping Beauty insertional mutagenesis screen identifies the pro-metastatic roles of CNPY2 and ACTN2 in hepatocellular carcinoma tumor progression. Biochem Biophys Res Commun. 2021;541:70–7.

[34] Li C, Guan R, Li W, et al. Analysis of myosin genes in HNSCC and identify MYL1 as a specific poor prognostic biomarker, promotes tumor metastasis and correlates with tumor immune infiltration in HNSCC. BMC Cancer. 2023;23:840.

[35] Sun J, Li S, Wang F, et al. Identification of key pathways and genes in PTEN mutation prostate cancer by bioinformatics analysis. BMC Med Genet. 2019;20:191.

[36] Zhao L, Fan W, Luo K, et al. Construction of a TTN mutation-based prognostic model for evaluating immune microenvironment, cancer stemness, and outcomes of colorectal cancer patients. Stem Cells Int. 2023;2023:6079957.

[37] Han X, Chen J, Wang J, et al. TTN mutations predict a poor prognosis in patients with thyroid cancer. Biosci Rep. 2022;42:1–14.

[38] Guo Q, Jian Z, Jia B, et al. CXCL7 promotes proliferation and invasion of cholangiocarcinoma cells. Oncol Rep. 2017;37:1114–22.

[39] Chen D, Ye Z, Lew Z, et al. Expression of NMU, PPBP and GNG4 in colon cancer and their influences on prognosis. Transl Cancer Res. 2022;11:3572–83.

[40] Shi K, Li N, Yang M, et al. Identification of key genes and pathways in female lung cancer patients who never smoked by a bioinformatics analysis. J Cancer. 2019;10:51–60.

[41] Xiong D, Pan J, Zhang Q, et al. Bronchial airway gene expression signatures in mouse lung squamous cell carcinoma and their modulation by cancer chemopreventive agents. Oncotarget. 2017;8:18885–900.

[42] Wang F, Han S, Yang J, et al. Knowledge-guided "Community Network" analysis reveals the functional modules and candidate targets in non-small-cell lung cancer. Cells. 2021;10:402.

[43] Wang YH, Shen CY, Lin SC, et al. Monocytes secrete CXCL7 to promote breast cancer progression. Cell Death Dis. 2021;12:1090.

[44] Desurmont T, Skrypek N, Duhamel A, et al. Overexpression of chemokine receptor CXCR2 and ligand CXCL7 in liver metastases from colon cancer is correlated to shorter disease-free and overall survival. Cancer Sci. 2015;106:262–9.

[45] Zhang N, Ng AS, Cai S, et al. Novel therapeutic strategies: targeting epithelial-mesenchymal transition in colorectal cancer. Lancet Oncol. 2021;22:e358–68.

[46] Dongre A, Weinberg RA. New insights into the mechanisms of epithelial-mesenchymal transition and implications for cancer. Nat Rev Mol Cell Biol. 2019;20:69–84.

[47] Al-Salam S, Sharma C, Afandi B, et al. BRAF and KRAS mutations in papillary thyroid carcinoma in the United Arab Emirates. PLoS One. 2020;15:e0231341.

[48] Heriyanto DS, Laiman V, Limantara NV, et al. High frequency of KRAS and EGFR mutation profiles in BRAF-negative thyroid carcinomas in Indonesia. BMC Res Notes. 2022;15:369.

[49] Ito Y, Miyauchi A, Fujishima M, et al. Prognostic significance of patient age in papillary thyroid carcinoma with no high-risk features. Endocr J. 2022;69:1131–6.

[50] Liu Q, Ma B, Song M, et al. Age-dependent changes in the prognostic advantage of papillary thyroid cancer in women: a SEER-based study. Clin Endocrinol (Oxf). 2023;99:342–9.